

Saint Petersburg State University

**Pastukhova Viktoriia Andreevna**

**Graduation work**

**METHANE FLUX DYNAMICS IN POLYGONAL  
TUNDRA INVESTIGATED BY THE EDDY  
COVARIANCE METHOD**

Main Scientific Direction 05.04.06.

”Ecology and Environmental Management”

”Cold Regions Environmental Landscapes Integrated Sciences (CORELIS)”

Scientific Supervisor: Dr. Irina V. Fedorova

Scientific Consultant: Prof. Dr. Lars Kutzbach

Scientific Consultant: Dr. Svetlana Y. Evgrafova

Revised by: Dr. Irina D. Grodnitskaya

Saint Petersburg

2018

**Scientific Supervisor:**

Dr. Irina V. Fedorova, Head of Geo-Ecology and Environmental Management Department, The Institute of Earth Sciences, Saint Petersburg State University, Saint Petersburg, Russia

**Scientific Consultants:**

Prof. Dr. Lars Kutzbach, The Institute of Soil Science, Hamburg University, Hamburg, Germany

Dr. Svetlana Y. Evgrafova, Senior Researcher at The V.N. Sukachev Institute of Forest, Siberian Branch, Russian Academy of Sciences, Krasnoyarsk, Russia

**Reviewer:**

Prof. Dr. Irina D. Grodnitskaya at The V.N. Sukachev Institute of Forest, Siberian Branch, Russian Academy of Sciences, Krasnoyarsk, Russia.

## Abstract

**Viktoriia A. Pastukhova**

Master Program for Cold Regions Environmental Landscapes Integrated Sciences  
"CORELIS" / 05.04.06. Ecology and Environmental Management

**Scientific Supervisor:** Dr. Irina V. Fedorova, Saint Petersburg State University

**Scientific Consultants:** Prof. Dr. Lars Kutzbach, Hamburg University;

Dr. Svetlana Y. Evgrafova, The V.N. Sukachev Institute of Forest

This study is dedicated to assessment of inter-annual methane flux dynamics in arctic polygonal tundra for the years of 2009-2017 in the Eastern Siberia, The Lena River Delta. This area is underlain by permafrost, which is huge carbon reservoir. Hence, the terrestrial arctic ecosystems are the largest natural source of atmospheric methane in the warming climate. As is well known, methane is a powerful greenhouse gas, thus, a significant driver for a climate change. The database we used in this study contains methane flux and meteorological parameters. Flux measurements were carried out with the eddy covariance technique provided nonintrusive spatially integrated high frequency data at the landscape scale. To assess inter-annual dynamics of methane emission it is necessary to identify processes triggered the emission. A multiple nonlinear regression analysis was applied to create a model, which describes the CH<sub>4</sub> flux. The most correlated drivers of methane emission were identified as friction velocity, soil temperature, air pressure, and relative air humidity (in the descending order of model parametric weight). The flux model was used for gap-filling with a further assessment of monthly averages and a calculation of cumulative summer methane fluxes for each year. The lowest cumulative summer methane flux was 1.28  $g/m^2$  (in 2017); the highest was 2.07  $g/m^2$  (in 2012). No clear indication of any upward trend was found; it seems that methane emission demonstrates annual fluctuations influenced by a variety of environmental parameters. Despite of the fact that our model is based mostly on meteorological parameters and is not precise enough, it has a practical significance; it is possible to use it as a tool for methane flux data conditioning in the future measurements.

## **Аннотация**

**Пастухова Виктория Андреевна**

Комплексное изучение окружающей среды полярных регионов «КОРЕЛИС» / 05.04.06. Экология и природопользование

**Научный руководитель:** к.г.н., доцент Федорова Ирина Викторовна, Санкт-Петербургский государственный университет

**Научный консультант:** профессор Ларс Кутцбах, Гамбургский университет; к.б.н., ст. науч. сотр. Евграфова Светлана Юрьевна, ФГБУН Институт леса им. В. Н. Сукачева СО РАН

Данное исследование посвящено оценке межгодовой динамики эмиссии метана в полигональной тундре на острове Самойловский в 2009-2017 гг. Район исследования расположен в Восточной Сибири в дельте р. Лены. Эта территория относится к зоне распространения многолетней мерзлоты, где сосредоточено большое количество органического углерода, способного при увеличении глубины сезонно-талого слоя выделяться в атмосферу в виде метана. Метан – сильный парниковый газ, оказывающий влияние на изменение климата, поэтому арктические тундровые экосистемы, являющиеся значительным естественным источником метана, требуют особого изучения. В нашем исследовании мы использовали данные, включающие в себя измерения потоков метана и микрометеорологических параметров. Поток метана был измерен с использованием метода вихревой ковариации. Для оценки межгодовой динамики эмиссии метана необходимо выявить факторы, влияющие на этот процесс. Для построения модели, описывающей поток метана, был использован метод множественной нелинейной регрессии. Наиболее значимыми факторами среды, влияющими на поток метана, были определены динамическая скорость ветра, температура почвы, давление и влажность воздуха. С помощью построенной модели были заполнены пропуски в имеющихся измерениях и оценены среднемесячные показатели и летные кумулятивные потоки метана с наименьшей эмиссией 1.28 г/м<sup>2</sup> в 2017г. и наибольшей 2.07 г/м<sup>2</sup> в 2012г. Средние оценки потоков демонстрируют межгодовые и сезонные флуктуации и отсутствие какого-либо тренда на возрастание или убывание. Практическая значимость разработанной модели заключается в возможности ее применения для заполнения пропусков в данных будущих измерений взамен метода обычной линейной интерполяции, который не отражает реальный природный процесс во всей его сложности.

# Contents

<b>1</b>	<b>Introduction</b>	<b>6</b>
<b>2</b>	<b>Materials and Methods</b>	<b>11</b>
2.1	Study Site . . . . .	11
2.2	Eddy Covariance Measurements . . . . .	12
2.2.1	Physical Basis of Eddy Covariance Method . . . . .	12
2.2.2	General Experimental Set-up and Eddy Covariance Data Processing . . . . .	16
2.3	Multiple Nonlinear Regression Analysis and Modeling . . . . .	19
2.3.1	Multiple Nonlinear Regression . . . . .	19
2.3.2	Stepwise Regression Approach . . . . .	19
<b>3</b>	<b>Results</b>	<b>21</b>
3.1	Environmental Conditions . . . . .	21
3.2	Methane Flux . . . . .	23
<b>4</b>	<b>Discussion</b>	<b>32</b>
<b>5</b>	<b>Conclusions</b>	<b>35</b>
<b>6</b>	<b>Acknowledgement</b>	<b>36</b>
	<b>Bibliography</b>	<b>37</b>

# 1 Introduction

Methane ( $\text{CH}_4$ ) is a powerful greenhouse gas (GHG) characterized by a high Global Warming Potential (GWP) in the atmosphere. It makes methane a significant driver for climate change (Denman et al., 2007). A number of recent studies concerning climatic changes is dedicated to quantification of methane emission from terrestrial arctic ecosystems, which are large natural source of atmospheric  $\text{CH}_4$ . The reason for this is permafrost, that underlies a major part of the Northern Arctic area. Permafrost is a huge carbon reservoir estimated at  $1300 \pm 200$  Gt in soils and deeper frozen sediments (Hugelius et al., 2014). Climate warming strongly influences the active layer thickness and distribution of permafrost. The thawing depth increase leads to changes in soil and hydrological conditions and, as a consequence, boosts the releasing of the soil carbon as GHGs, particularly, carbon dioxide and methane, thus these processes induce further climate warming (Frolking et al., 2013).

The contribution of the Arctic wetlands and tundra to the natural methane emission accounted for 20% (up to 1 Gt) of  $\text{CH}_4$  per year to the global  $\text{CH}_4$  budget (Arora et al., 2015; Prather et al., 2001; Walter et al., 2001; Christensen et al., 1996). Nowadays with a strong emphasis on climate change the GHG budget of Arctic wetlands has attracted great attention of researchers.

The impact on the GHG budget of tundra landscapes is attributed to the high relative radiative forcing of  $\text{CH}_4$ , which is 25 times greater compared to  $\text{CO}_2$  (for the scale of 100 years) (Solomon, 2007). Therefore, these methane-emitting landscapes could be an effective GHG source even if they are removing  $\text{CO}_2$  from the atmosphere (Wille et al., 2008; Whiting and Chanton, 2001). Most of the previous investigations of source strength, rate and driving forces of  $\text{CH}_4$  flux in wet polygonal tundra were carried out by closed-chamber technique. That approach does not provide precise information for landscape scale methane emission because of high spatial and temporal  $\text{CH}_4$  flux fluctuations (Zhang et al., 2012; Sachs et al., 2008b). In order to get broad picture of entire ecosystem processes the most promising method is eddy covariance measurements. This technique provides integrated high-frequency data for continuous period at the landscape scale for better analysis of entire ecosystem exchange processes. To the extent of our knowledge there are no studies reported long-term inter-annual methane flux observations in polygonal tundra using eddy

covariance technique. Although, a few papers reported eddy covariance data of CH<sub>4</sub> emission in Siberian Arctic tundra landscape for the entire snow-free period within the one or two years, e.g. for the years of 2003-2004 (Wille et al., 2008) and 2006 (Sachs et al., 2008); and cold season CH<sub>4</sub> emission in North Alaska using eddy covariance for the years of 2013-2015 (Zona et al., 2016). The emission rates and driving forces of methane fluxes in polygonal tundra warrant further investigation. This study is dedicated to long-term inter-annual CH<sub>4</sub> flux dynamics using eddy covariance technique as a reliable method to assess ecosystem exchange variability. Approximately  $22.79 \times 10^6$  km<sup>2</sup> or 23.9% of the exposed land surface area in the Northern Hemisphere underlain by permafrost (excluding ice sheets and glaciers). The term “permafrost” is based on temperature and defined as ground (soils, sediments or rocks, including organic material) that remains at or below 0 °C for more than two years (Zhang et al., 2008). The temperature of the ground surface (Ground or Soil Temperature Regime) in permafrost regions highly influences the spatial distribution, thickness and temperature of permafrost; the seasonal differences in temperature are decreasing with the soil depth. The near-surface soil layer in permafrost regions, which experiences positive temperature during the summer season, is called supra-permafrost layer. The uppermost soil layer which seasonally freezes and thaws is defined as active layer (French, 1996).

The climate is the dominating factor determining the existence of permafrost. Long term rise of air temperature in the arctic regions makes the active layer thickness grow, thus previously permanently frozen ground becomes unfrozen. According to Hugelius et al. (2014) carbon storage in the permafrost regions is estimated at  $1300 \pm 200$  Gt in soils and deeper frozen sediments. With the deepening of the active layer more and more previously frozen organic carbon becomes available for decomposition (Sachs et al., 2008). This is the major reason why arctic tundra ecosystems are characterized by high sensitivity to climate change and simultaneously strongly influence the global GHG budget.

Polygonal tundra landscapes are formed in permafrost conditions of the arctic regions. Polygons are formed by the thermal-contraction-cracking process. During the winter period hard frost leads to the formation of cracks due to thermal contraction of the frozen ground. Such cracks penetrate to the deep permafrost sediments. During the spring period melt water flows in to the open frost crack and freezes

next winter. This process repeats year by year, and as a result, an almost vertical vein, later an ice wedge, is formed. Under the harsh climatic conditions in the arctic regions, the thermal-contraction-cracking process with ice wedges developing takes place almost every year leading to ice wedges expansion and polygonal tundra landscape formation (French, 1996).

Wetland soils are contributors to atmospheric methane due to microbial decomposition of organic material contained in these soils. A special group of microorganisms, methanogens (methanogenic bacteria), is responsible for  $\text{CH}_4$  production in a wet anaerobic environment. The formation of methane is a complex set of natural ecosystem processes, which starts with the primary fermentation of organic macromolecules to acetic acid, other carboxylic acids, alcohols, carbon dioxide, and hydrogen. The primary fermentation is followed by the secondary fermentation of the alcohols and carboxylic acids to acetate, hydrogen, and carbon dioxide. A full conversion of these substances to methane is completed by methanogenic bacteria (Zhuang et al., 2004).

Soils have a potential both for methane production and methane consumption processes. The  $\text{CH}_4$  production occurs in anaerobic conditions, whereas the consumption (oxidation) is possible in aerobic part of the soil. The net  $\text{CH}_4$  release from wetland soils is a result of both processes competing and is also affected by the gas transport (Jahn et al., 2010).

There are three different methane transport mechanisms from the soil to the atmosphere (Figure 1). The first way is plant-mediated, when  $\text{CH}_4$  reaches the atmosphere by a conductive flow through vascular plants by a well-developed special tissue called aerenchyma. The second way is diffusion, and the last one is ebullition, that is bubbles issuing from the soil (Whalen, 2005).

It is well-known that methane concentration in the atmosphere has been increasing during the industrial period due to high anthropogenic emission. Since the middle of 1980s  $\text{CH}_4$  concentration in the atmosphere has decreased and the growth rate kept around zero over 1999-2006 (Arora et al., 2015; Prather et al., 2012). According to Bousquet et al. (2012) a remarkable increase in methane in 2007 at high northern latitudes is believed to be triggered by increased emissions from arctic wetlands due to changing meteorological conditions. This fact is considered to be



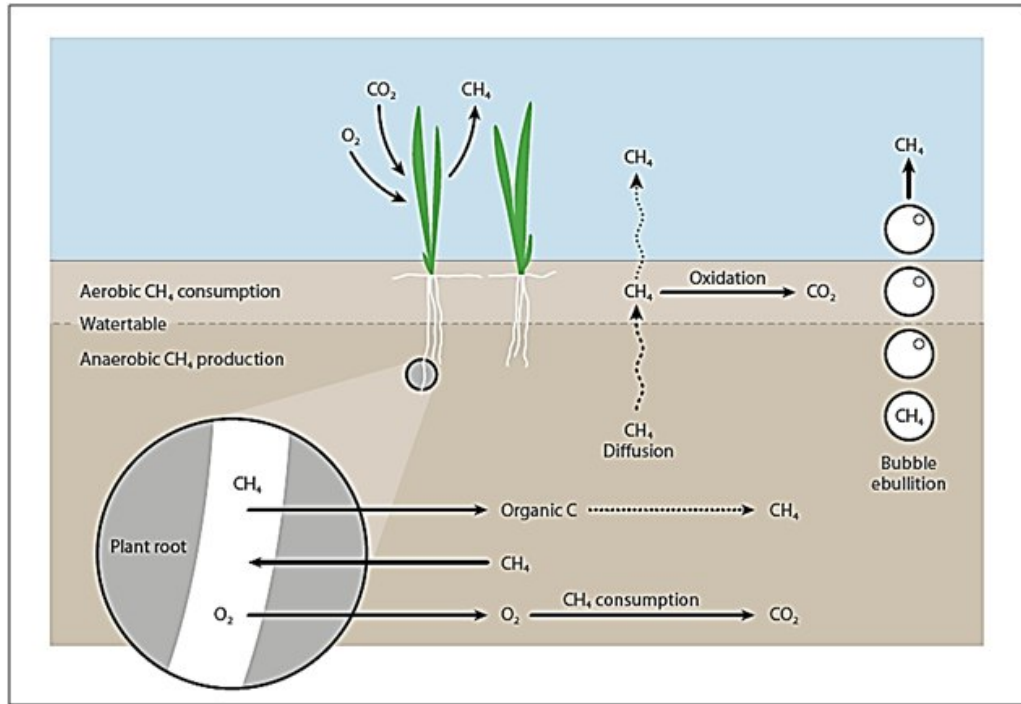


Figure 1: Methane transport mechanisms (Chesworth, 2008)

a consequence of anthropogenically-caused global warming, which lead to substantial natural emission enhancement in high latitudes (Arora et al., 2015). Therefore the emission rates and driving forces of methane fluxes in arctic polygonal tundra inspired further investigations in recent years.

Permafrost conditions and spatial heterogeneity are two major challenges for methane flux estimation in the Arctic. Measurements covering a whole year are fairly rare and the majority of existing studies is based on growing season measurements only. Long-term investigations of  $\text{CH}_4$  fluxes for Siberian polygonal tundra on ecosystem scale mostly cover only two or three years (e.g. Sachs et al. (2008), Wille et al. (2008)). Here we present a study based on long-term methane flux observations from the Lena River Delta which cover the period of 2009-2017.

The objective of this study is to assess the dynamics of inter-annual  $\text{CH}_4$  emission from tundra landscapes during nine recent years (2009-2017) and identify processes which may trigger the methane emission. We have used eddy covariance methane

flux data combined with meteorological and soil temperature observations carried out in Siberian polygonal tundra, the Lena River Delta, Samoylov Island. As it was mentioned before, the terrestrial Arctic ecosystems are considered as a large natural source of atmospheric  $\text{CH}_4$ .

Thus, this study aims at investigating  $\text{CH}_4$  emission rate trends within the period 2009-2017; in case a growing trend exists we could infer that this region will considerably amplify the global long-term  $\text{CH}_4$  emission.

The objectives of this study were to:

1. estimate data availability (methane flux and meteorological parameters) for the years of 2009-2017;
2. choose the target research periods;
3. apply multiple nonlinear regression analysis to create the model;
4. apply the model to fill the gaps of the data;
5. determine and describe the environmental drivers of  $\text{CH}_4$  emission;
6. assess the integrated  $\text{CH}_4$  emission over target research periods;
7. assess the inter-annual  $\text{CH}_4$  emission dynamics.

## 2 Materials and Methods

### 2.1 Study Site

The investigation area is located on Samoylov Island ( $72^{\circ}22'N, 126^{\circ}30'E$ ), 120 km southwards from the Arctic Ocean in the southern-central part of the Lena River Delta. The Lena River Delta is the largest arctic delta system within the circum-arctic land masses, which occupies the area of about 32000 km<sup>2</sup>. The delta represents a vast network of river channels and more than 1500 islands, which form three main geomorphological terraces. The entire area is situated in the continuous permafrost zone (with a permafrost thickness up to 600 m and mean annual temperature of about  $-8.6^{\circ}\text{C}$  (at 10.7 m depth)) and presents a landscape typically covered by the patterned ground of ice wedge polygons in different stages of development (Hubberten et al., 2006; Are and Reimnitz, 2000; Boike et al., 2013).

Samoylov Island has an area of 7.5 km<sup>2</sup> and can be divided into two geomorphological units: western and eastern parts. The western part is a modern floodplain (annually flooded in spring) with the elevation of 1 – 5 m a.s.l. The eastern part represents the Late-Holocene river terrace (partly flooded during extreme flooding only) with the elevation of 10 – 16 m a.s.l. (Kutzbach, 2006).

The climate of this territory is true-arctic, continental and is characterized by a low annual air temperature ( $-14.7^{\circ}\text{C}$ ) and low precipitation (annual mean 199 mm). The duration of winter season is about nine months (from the end of September to the end of May) with the average and minimum temperature  $-30^{\circ}\text{C}$  and  $-48^{\circ}\text{C}$  respectively (Hubberten et al., 2006). The snowmelt typically starts in the beginning of June and is followed by the growing season which lasts from the middle of June to the middle of September (Boike et al., 2008).

The well-structured microrelief of the island is caused by the development of low-centred ice-wedge polygons with a diameter of about 20 m. The depressed centres of these polygons are surrounded by elevated rims (with the typical elevation difference of 0.5 m). Typical soil types in the wet centres are Typic Historthels, whereas at the dryer polygon rims dominate Glacic or Typic Aquiturbels (Soil Survey Staff, 1998). Hydrophytic sedges and mosses are the major vegetation types in the poly-

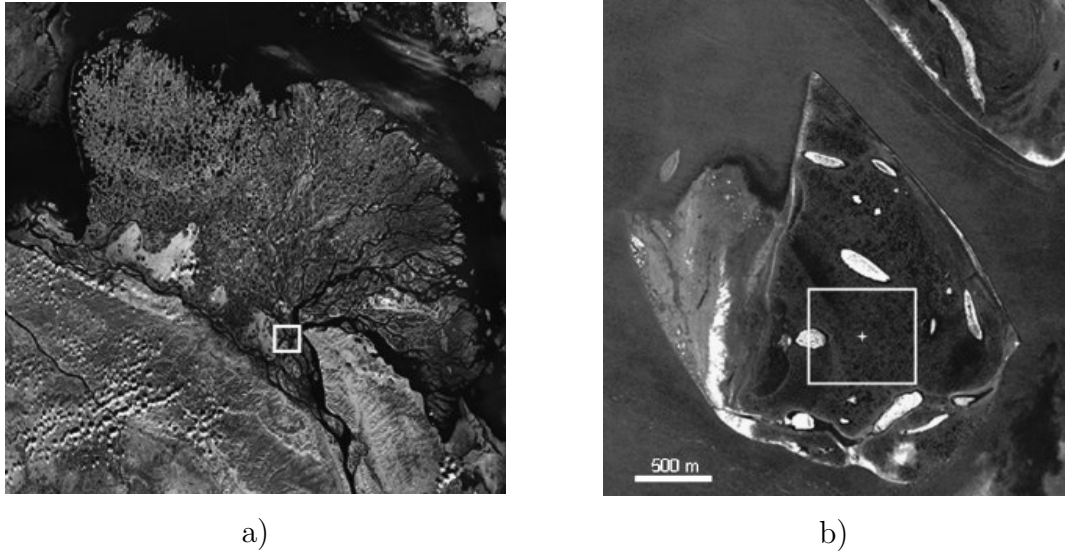


Figure 2: Satellite image of a)the Lena River Delta and b)Samoylov Island (Wille et al., 2008)

gon centres and their edges. The vegetation dominating the rims is represented by mesophytic dwarf shrubs, forbs, and mosses (Kutzbach et al., 2003).

## 2.2 Eddy Covariance Measurements

### 2.2.1 Physical Basis of Eddy Covariance Method

The eddy covariance is a micrometeorological method to measure atmospheric parameters and calculate vertical turbulent flux within the atmospheric boundary layer. This technique provides spatially integrated high frequency wind velocity vector and atmospheric scalar data series in the landscape scale. Eddy covariance is widely applied to determine exchange rates of trace gases and energy fluxes over different natural and agricultural landscapes and to quantify atmospheric gas emissions from land and water areas.

The major advantage of the eddy covariance method is quasi-continuous direct measurements of the land-atmosphere fluxes (momentum, energy and mass) over a broad area (several  $\text{km}^2$ ), which are provided *in situ* and do not disturb investigated ecosystem. The eddy covariance measures the flux at the time scale of about half an hour

and yields so-called quasi-continuous data. In fact the measurements are not continuous; due to some specific weather conditions and the equipment failures gaps in the time series can occur (Burba, 2013).

Despite of all the advantages it is not easy to apply this technique. First, prior to the eddy covariance system mounting it is necessary to determine the area of interest, which should be a homogeneous terrain without strong advection/convection air movement, then evaluate the height of the tower. Second, calculation of the real flux needs a set of mathematical and physical assumptions. Third, flux data series must be corrected in order to mitigate measurement faults, mismatches due to sensors separation and as a consequence over- or underestimation of the flux (Aubinet et al., 2013).

Nevertheless, eddy covariance technique is considered to be the most accurate and reliable way to study ecosystem exchange processes, and can be applied to determine emission and consumption rates of various gases and water vapor and to estimate the ecosystem carbon balance (Burba, 2013).

The concept of the atmospheric eddy transport is the following: air flow can be considered as a horizontal flow of many rotating eddies. Each eddy is characterized by 3-dimensional components, including vertical movement of the air, which can be directly measured from the eddy covariance tower (Burba, 2013).

In micrometeorology, flux is defined as the amount of any properties (e.g. substance  $s$ ) transported per unit area per unit time. It is stated that vertical flux in turbulent flow is equal to a mean product of air density  $\rho_d$ , vertical wind speed  $w$ , and the dry mole fraction (mixing ratio)  $s$  of the gas of interest:

$$F = \overline{\rho_d w s} \quad (1)$$

The sign of the covariance indicates the direction of the turbulent transport: “plus” means upward, “minus” means downward flux.

The next step is Reynolds decomposition, which is necessary because in reality it is difficult to achieve needed accuracy for measurements of  $s$  and especially  $w$  at sufficient frequency. Reynolds decomposition is used to break terms into means and deviations:

$$F = \overline{(\overline{\rho_d} + \rho'_d)(\overline{w} + w')(\overline{s} + s')} \quad (2)$$

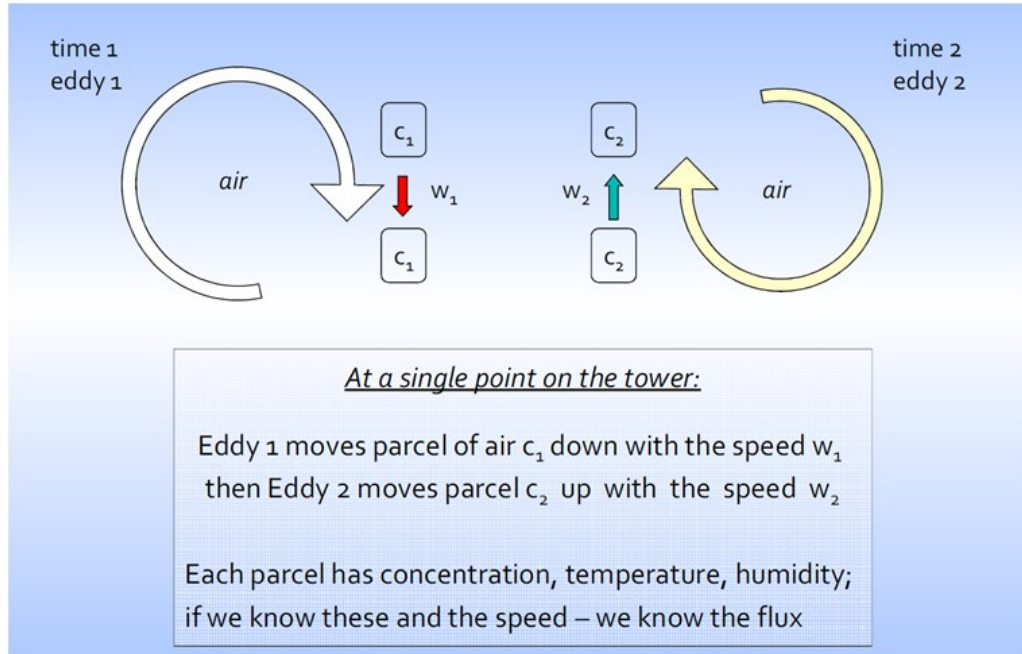


Figure 3: Turbulent transport: Moving air parcels that contain gas molecules (Burba, 2013)

To simplify of the equation (2) the following statements have to be asserted true (Burba, 2013):

- average fluctuations equal zero by definition;
- air density fluctuations assumed to be negligible;
- mean vertical velocity assumed to be negligible for horizontal homogeneous terrain (no divergence/convergence)

Finally, simplified flux equation is:

$$\overline{F} = \overline{\rho_d} \times \overline{w's'} \quad (3)$$

where  $w's'$  is a covariance of fluctuations of vertical wind speed and fluctuations of gas concentration.

The surface exchange (material or energy) calculation needs an assumption that flux measured at height  $h_m$  equals the surface flux. The connection between surface exchange and turbulent flux of a scalar quantity  $s$  is achieved by integrating over an

arbitrary control volume of the one-point time averaged conservation equation (4), the integral scalar budget equation.

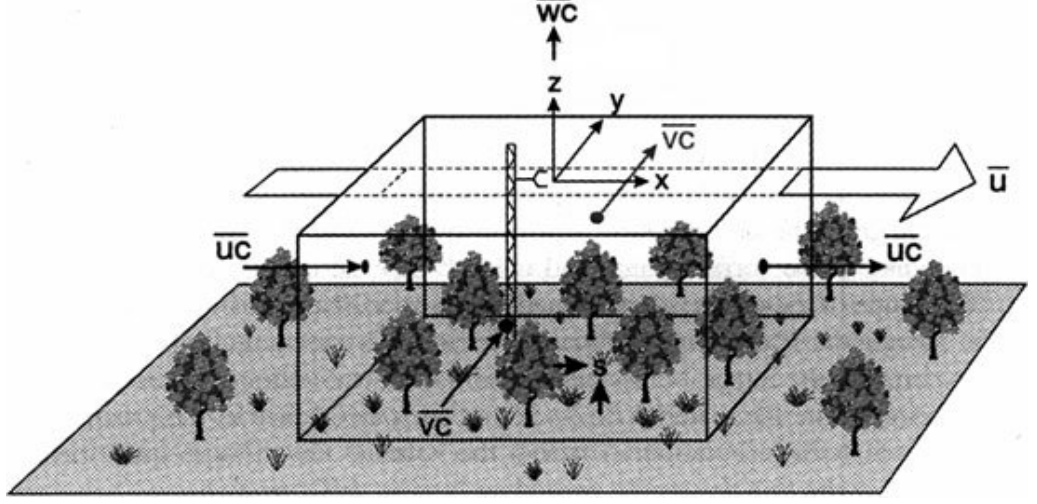


Figure 4: Schematic image of integration over a control volume in homogeneous terrain (Aubinet et al., 2013)

$$\begin{aligned} \frac{1}{4L} \int_{-L}^L \int_{-L}^L \int_0^{h_m} & \left[ \underbrace{\frac{\partial \chi'_s}{\partial t}}_I + \underbrace{\bar{u} \frac{\partial \chi'_s}{\partial x} + \bar{v} \frac{\partial \chi'_s}{\partial y} + \bar{w} \frac{\partial \chi'_s}{\partial z}}_{II} + \underbrace{\frac{\partial \bar{u}' \chi'_s}{\partial x} + \frac{\partial \bar{v}' \chi'_s}{\partial y}}_{III} + \underbrace{\frac{\partial \bar{w}' \chi'_s}{\partial z}}_{IV} \right] dz dx dy = \\ & = \frac{1}{4\rho L^2} \int_{-L}^L \int_{-L}^L \int_0^{h_m} \left[ \underbrace{\bar{S} dz dx dy}_V \right] \end{aligned} \quad (4)$$

This equation is integrated both horizontally over the area of interest,  $A$  ( $2L \times 2L$ ), and vertically, from surface to the measurement height  $h_m$ , where  $\chi_s$  is mass mixing ratio of the constituent  $s$  to the mass of dry air and  $u'$ ,  $v'$  and  $w'$  are longitudinal, lateral and vertical components respectively (Aubinet et al., 2013).

The equation (4) can be simplified using the assumption that the measurement system is placed in a horizontally homogeneous equilibrium layer where all horizontal gradients are negligible (II and III). In homogeneous surface layer the net ecosystem exchange (NEE) is equal to the sum of turbulent flux (IV) and storage change flux (I), thus in stationary conditions it can be expressed by the following equation:

$$\bar{w}' \chi'_s |_{h_w} = NEE \quad (5)$$

The equation (5) is a physical basis of micrometeorological method for measuring surface exchange (Aubinet et al., 2013).

### **2.2.2 General Experimental Set-up and Eddy Covariance Data Processing**

The datasets used in this study were obtained from Prof. Dr. Lars Kutzbach Research Group, Institute of Soil Science, Hamburg University. Data include methane fluxes, micrometeorological parameters (air temperature, air pressure, relative humidity, wind speed) and soil temperature measurements. The eddy covariance system tower (ECS) is located in the eastern part of Samoylov Island. ECS tower is surrounded by a relatively homogenous footprint area of wet polygonal tundra (larger water bodies are located at a 600 m radius around the tower).

The measurements were carried out at the same location for the period of 2009-2017 years. Methane concentration measurements were provided with a closed-path CH<sub>4</sub> analyzer DLT-100, Los Gatos Research, USA (2009-2010 years); and with an open path CH<sub>4</sub> analyzer LI-COR, LI-7700 (2011-2017 years). The wind speed was measured with a 3-dimensional sonic anemometer (Solent R3, Gill Instruments Ltd, Lymington, UK) fixed on the 3 m ECS tower, at the height of 3.65 m. The gas analyzer sample point was 15 cm under the anemometer measurement point. The air temperature, relative humidity and barometric pressure measurements were also provided by the ECS tower. The soil temperatures were measured near the tower at the depth of 7 cm in the polygonal center. The measurements were carried out every half of an hour.

The eddy covariance raw data have to be processed to determine land-atmosphere CH<sub>4</sub> fluxes. The processing has been applied for each 30-minutes averaging period. The approach of eddy covariance data processing consists of two steps, which are the preliminary processing of the raw measurements and the flux computations. The first step includes sonic anemometer tilt correction and time lag compensation correction.

1. The sonic anemometer tilt correction using two-step coordinate rotation. Because



Table 1: Data availability of the methane flux, meteorological and soil temperature measurements with the corresponding time periods

N	Measured parameter	Recording periods (summer months)								
		2009	2010	2011	2012	2013	2014	2015	2016	2017
1	Methane flux	07-08	08	06-08	07-08	06-08	06-08	06-08	06-08	06-08
2	Air temperature	07-08	06-08	06-08	06-08	06-08	06-08	06-08	06-08	06-07 08
3	Air pressure	07-08	06-08	06-08	06-08	06-08	06-08	06-08	06-08	06-07 08
4	Relative humidity	07-08	06-08	06-08	06-08	06-08	06-08	06-08	06-08	06-07 08
5	Wind speed	07-08	08	06-08	07-08	06-08	06-08	06-08	06-08	07 08
6	Soil temperature	06-08	06-08	06-08	06-08	06-08	06-08	06-08	06-08	06-08

the sonic anemometer can not be aligned to be exactly perpendicular to the mean flow streamlines, the vertical wind  $w$  is affected by the signal of horizontal wind, that leads to distortion of the flux  $\overline{w's'}$ . Double coordinate rotation includes first (around  $w$ -axis to reduce mean  $v$  to zero) and second (around  $v$ -axis to reduce mean  $w$  to zero) rotations. Two-step coordinate rotation has been performed on the wind components measured by the sonic anemometer. Mean transverse and vertical wind have to be reduced to zero (Wilczak et al., 2001; Burba, 2013).

2. Time lag compensation. Due to spatial separation of the anemometer and gas analyzers or transport of sample air through a tube the time lag occurs and has to be eliminated before the calculations. The delays between the time series of vertical wind and  $\text{CH}_4$  - concentration have been determined applying covariance maximization method (find of the time shift, where the covariance reaches a maximum using cross correlation function). These lags have been removed for the whole averaging period (Burba, 2013; Mauder and Foken, 2015).

The second step is the raw flux computations, which includes the calculation of the raw  $\text{CH}_4$  flux using the equation (3), the flux spectral corrections of low and high frequency range and the quality flag calculation correction of the  $\text{CH}_4$  fluxes (Foken and Wichura, 1996; Mauder and Foken, 2015). Density (WPL) correction and frequency response correction are necessary to be applied make raw fluxes reliable for the further analysis.

1. Density (WPL) correction is necessary to apply because in fact  $w$  is not equal to zero due to air density fluctuations. Density correction compensates for the effects of air density fluctuations on measured fluctuations of atmospheric gases, e.g.  $\text{H}_2\text{O}$ ,

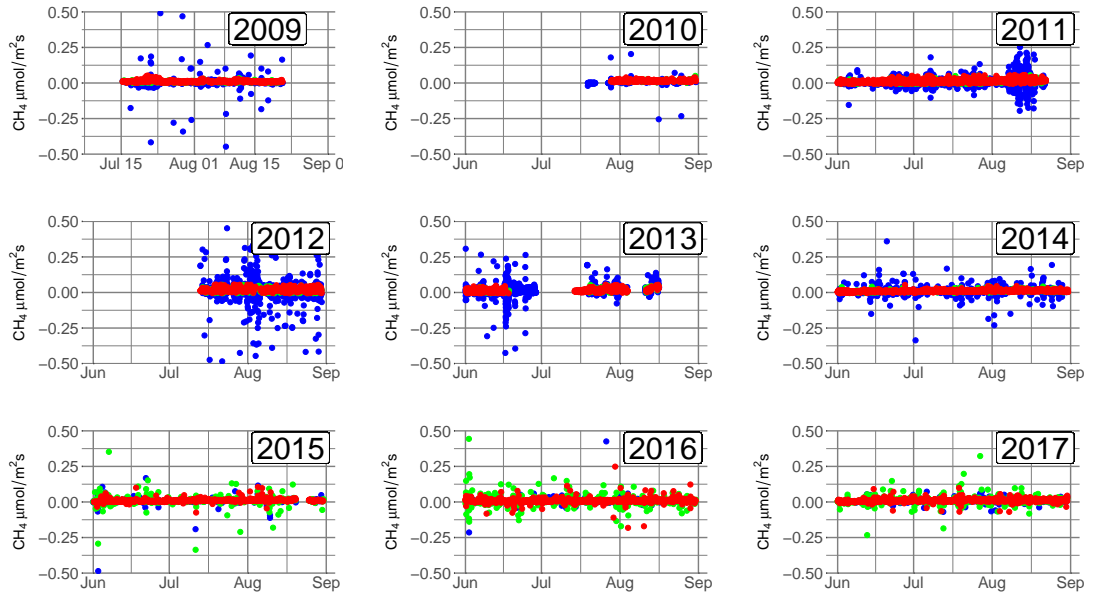


Figure 5: Flux data availability during the summers of the 2009-2017 years (June-August); red dots mark the best quality data (flag “0”), green for middle quality (flag “1”) and blue for the worst quality emissions (flag “2”).

$\text{CH}_4$ ,  $\text{CO}_2$  (Webb, Pearman, Leuning (1980): “WPL correction”). Applying this correction two main problems of air density fluctuation can to be solved: water vapor dilution and thermal expansion of the gas (Webb et al., 1980; Burba, 2013).

2. Frequency response correction. The necessity of applying frequency response correction occurs due to flux attenuation. The eddy covariance measurement system can not detect the full range of turbulent exchange, because of limited spatial or temporal resolution, attenuation of amplitude of scalar quantities and mismatch of spectral or spatial properties. Attenuation properties are described by transfer functions using transformation of a function or discrete time series between the time domain and the frequency domain and back applying Fourier transformation and frequency response corrections (Burba, 2013).
3. After processing of the raw  $\text{CH}_4$  fluxes, they have to be divided into three quality groups. The quality flag separation was carried out with two quality control tests. The best quality measurements with the flag “0” should be used for a more precise analysis of the emission, the quality flag “1” measurements are appropriate for a general analysis, and the measurements with the flag “2” have the worst quality

and should not be taken into account (Mauder and Foken, 2015).

## 2.3 Multiple Nonlinear Regression Analysis and Modeling

### 2.3.1 Multiple Nonlinear Regression

In statistics, nonlinear regression is defined as a form of regression analysis in which the relationship between dependent (or response) variable  $y$  and independent (or explanatory) variable  $x$  is modeled by a nonlinear function. The case of more than one explanatory variable is called multiple nonlinear regression and can be expressed by the general equation (6) (Demyanov and Saveleva, 2000).

$$y = f(x_1, x_2, x_3, \dots, x_n) \quad (6)$$

We will use multiple nonlinear regression analysis as a tool to determine the environmental drivers of the emission. The method could be described by the equation (6), where  $y$  is a response variable and  $x_1, x_2 \dots x_n$  are explanatory variables. In our model the response variable is CH<sub>4</sub> flux and the explanatory variables, which influence the flux, are environmental parameters.

### 2.3.2 Stepwise Regression Approach

In order to determine the variables, which have influence on CH<sub>4</sub> flux and should be included in the model, we will apply stepwise regression. The stepwise regression is an automated process based on continuous adding and removing variables from the model according to the results of t-statistics of their estimated coefficients. The decision to add or remove a variable is based on the threshold values of F-statistic (with the significance level of 5%). This procedure yields the best subset of independent variables.

Stepwise regression can be implemented in three ways, which are the forward selection, backward and bidirectional elimination. Forward selection is the process of

improving initially empty model by stepwise adding of variables, one by one, until no more input variables can improve the model. The backward elimination works in the opposite direction. It starts with a full model (all variables are used in the model) by rejecting the variables that are least significant for the model, one by one, till no more removals can improve the model. The bidirectional elimination is a combination of these two approaches, i.e. it is similar to the forward selection, but with the opportunity to remove selected variables on each step. In this study we use the bidirectional elimination to build the model.

However, the stepwise regression analysis has some issues; one of them is multicollinearity (relations between selected independent variables), which can strongly influence the result of the analysis. In spite of well-described relations between the environmental parameters and CH<sub>4</sub> fluxes, it is necessary to control the order of variables added or removed and discern which variable should be rejected or included. As a result of this analysis we obtain a model which can be used for gap-filling and further interpretation of the processes which control the CH<sub>4</sub> emission.

We use R-Studio (R Core Team, 2013) for statistical processing, modeling and further data gap-filling procedures.

### 3 Results

#### 3.1 Environmental Conditions

The summer air temperature over the years 2009-2017 varies from 5 °C in June to 14 °C in July. The highest air temperatures were observed for July (6 – 14 °C), the lowest – for June (5 – 7 °C). During the study period the warmest year was 2010, while 2013, 2015 – 2017 were the coldest. High air temperatures in July and August are due to the advection of warm continental air from the South (Wille et al., 2008).

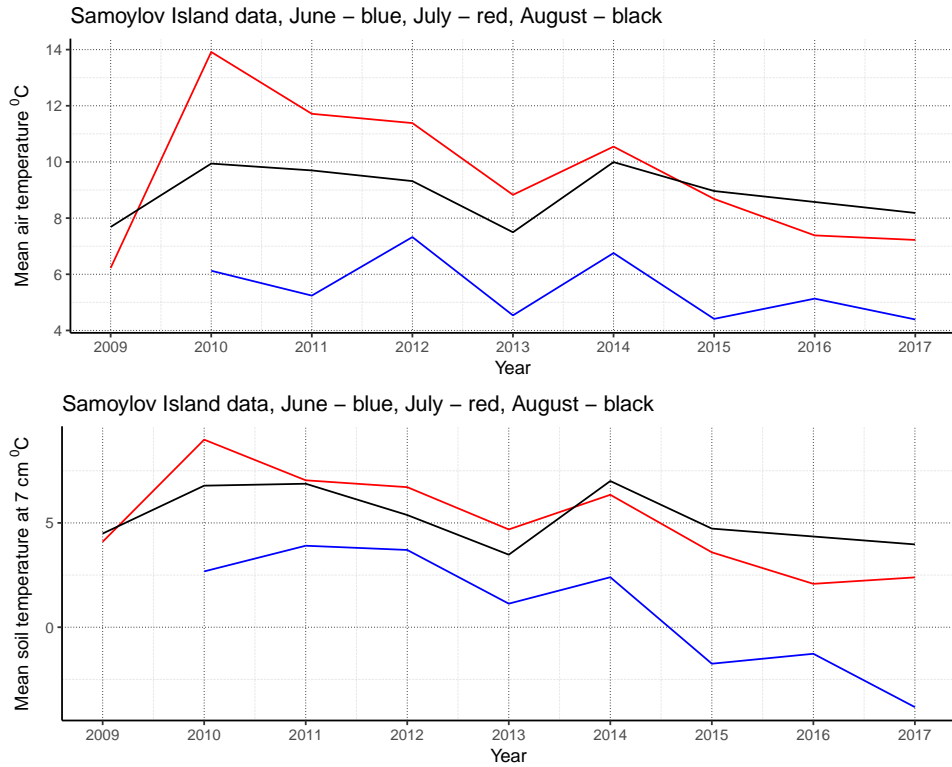


Figure 6: Meteorological parameters for 2009-2017: monthly averages for air temperature and soil temperature (at 7 cm depth, polygon center).

The soil temperature dynamics (at 7 cm depth, wet polygon center, Figure 6) follows the air temperature and demonstrates the highest value for 2010 and 2014 (9 °C and 6 °C in July, respectively). The years of 2013, 2015 – 2017 characterized by a lower

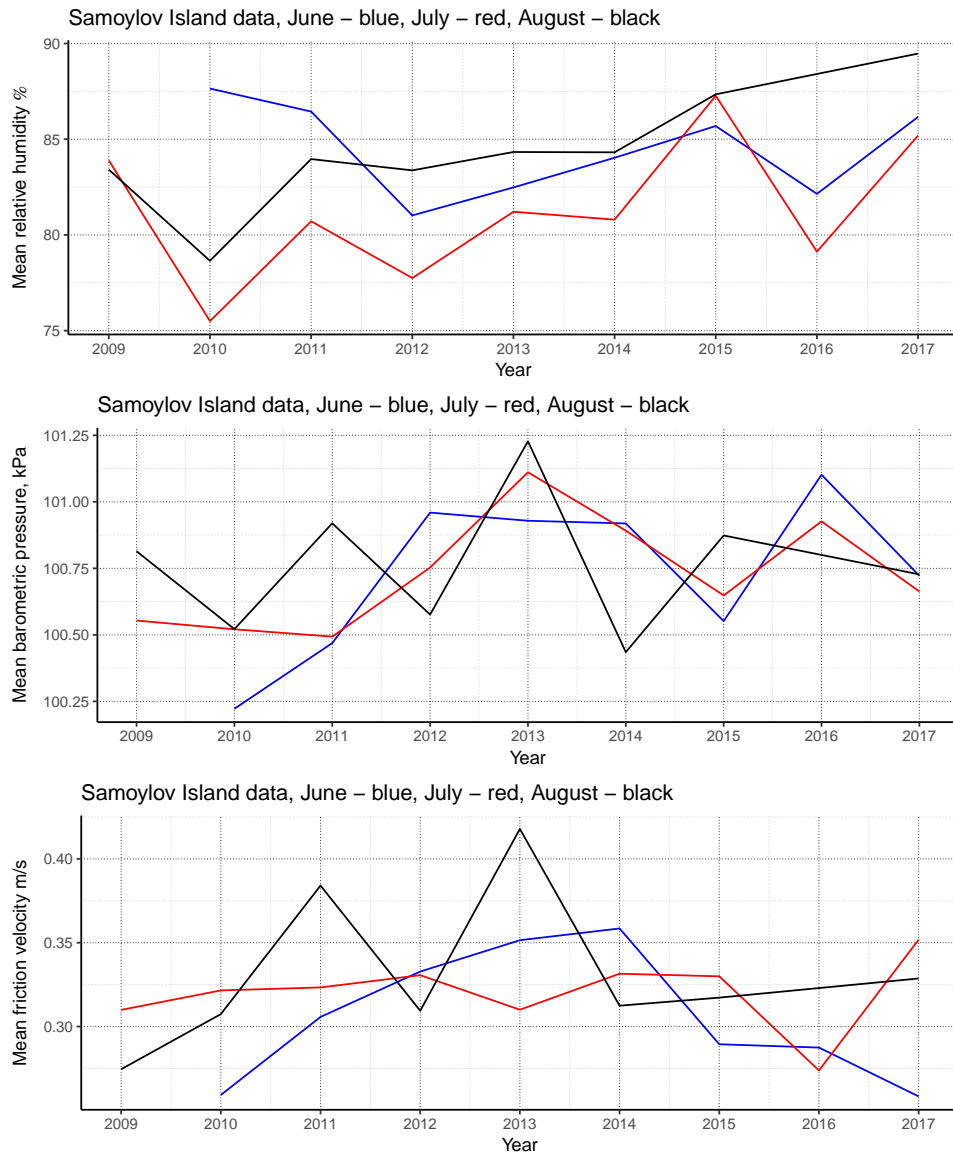


Figure 7: Meteorological parameters for 2009-2017: monthly averages for relative air humidity, air pressure and near-surface turbulence (friction velocity).

soil temperature (even frozen during June 2015 – 2017).

The relative humidity (Figure 7) shows no clear seasonal dynamics and demonstrates different monthly peaks for different years. Precipitation measurements were also analyzed, but were not included into the model and further analysis due to large amount of gaps in rainfall time series each year. We decided to choose relative

air humidity as an indicative factor of general water content in the environment. Maximum values of relative humidity were measured in 2015 and 2017; the driest month was July nearly in all years with a minimum in 2010 and 2012 (76% and 78% respectively).

Mean air pressure varies from 100.25 to 101.20 kPa during the summers 2009 – 2017 and demonstrates no seasonal dynamics within each year. The same is true for friction velocity. Near-surface turbulence (friction velocity) was used in this study as a factor describing atmospheric flows characteristics of near-surface boundary layer and closely correlates with wind speed.

### 3.2 Methane Flux

The emission of methane is boosted or inhibited by a variety of environmental parameters, which can have a linear or exponential influence. Each parameter modulates the overall emission so it can be presented best as a product of functions depending on each environmental parameter. A number of recent studies have reported the modeling approach based on multiplicative nonlinear regression modeling, where the methane flux is approximated as a product of an ecosystem reference flux and a set of environmental parameters, each has its specific regulation factor (Friborg et al., 2000; Wille et al., 2008; Sachs et al., 2008; Franz et al., 2016). For consistency an exponential model was chosen for the regression analysis; the case when a parameter is a factor in resulting product can be identified in the exponential model as a coefficient that is near to unity. In a general form this equation can be written as:

$$y = a_1^{x_1} * a_2^{x_2} * a_3^{x_3} * \dots * a_n^{x_n} \quad (7)$$

Where  $a_i$  are model coefficients and  $x_i$  are environmental parameters (or variables). The stepwise regression analysis was started with 8 variables, which are the air temperature ( $T_{air}$ ), the soil temperatures ( $T_{soil_2}$ ,  $T_{soil_4}$ ,  $T_{soil_7}$ ,  $T_{soil_8}$ ), the relative air humidity ( $RH$ ), the air pressure ( $p_a$ ) and the near-surface turbulence (friction velocity  $u^*$ ). These variables have to be unified (corresponding means are subtracted and constant correction factors are introduced) for the consistency of all the used parameters prior to including them into the model. Our model has an exponential

character and large exponent values make the model less stable; consequently, less reliable. In order to avoid such behavior the parameters have to be normalized in the following way. The air and soil temperatures are included into the model as a difference between a measured value and the average value over each measurement period divided by 10 degrees  $((T - \bar{T})/10)$ . Relative humidity is converted from per cent to ratio (1 is 100%,  $rRH$ ). Air pressure and friction velocity are included as differences between a measured value and the average value over each measurement period  $(p_a - \bar{p}_a, u^* - \bar{u}^*)$ . These transformations do not change the behavior of the model, but change the coefficient in front of the final product and enhance the model readability.

We applied the stepwise procedure for each year and analyzed the variables, which were more frequently selected as a significant. Then we rejected the variables, which were not included to the model or did not significantly improve it.

Table 2: Assessment of the inter-annual contribution of environmental variables using stepwise approach (blue colour marks sets of parameters for each year).

Year	$T_a$	$P_a$	rRH	$u^*$	$T_{s_2}$	$T_{s_4}$	$T_{s_7}$	$T_{s_8}$
2009								
2010								
2011								
2012								
2013								
2014								
2015								
2016								
2017								

The result of this assessment is the final regression model, which includes the following explanatory variables: soil temperature at 7 cm depth ( $T_{soil_7}$ ), relative humidity ( $RH$ ), air pressure ( $p_a$ ) and near-surface turbulence (friction velocity  $u^*$ ).

In order to get a subset of explanatory variables, which provide the most reliable parameters for our model to describe the functional relationship between  $CH_4$  flux and its environmental drivers, the dependence between  $CH_4$  flux and environmen-



tal variables was analyzed. The model parameters based on these variables is then used for gap-filling and extrapolation. For this analysis daily averages of CH<sub>4</sub> flux were calculated, and its errors were calculated as standard errors of the mean. A noticeable CH<sub>4</sub> flux dependence on friction velocity, soil temperature at 7 cm depth (polygon center), air pressure and relative humidity was found. These four variables were included in the model following the approach of Friberg et al. (2000) also applied by Sachs et al. (2008) and Wille et al. (2008). An agreement between measured and modeled fluxes is the best described when the flux is modeled as:

$$FCH_4 = a * b^{(u^* - \bar{u}^*)} * c^{[(T - \bar{T})/10]} * d^{(rRH)} * e^{(p_a - \bar{p}_a)} \quad (8)$$

In this equation FCH<sub>4</sub> is measured methane flux,  $a$ ,  $b$ ,  $c$ ,  $d$  and  $e$  are the coefficients determined by the fit process (Table 3). Equation (8) was applied to fill the gaps of the daily CH<sub>4</sub> flux time series over each summer season for the years of 2009 – 2017. During the analysis the error of modeled daily fluxes was calculated as a relative average deviation ( $rad, \%$ ) of the fit residuals.

$$rad = \frac{\sqrt{\sum_i^n ((modeled FCH_4)_i - (measured FCH_4)_i)^2}}{n \times \overline{measured FCH_4}} \quad (9)$$

Where  $i$  denotes index of each time period bin used for calculation of modeled  $FCH_4$  and  $n$  is a total number of these periods. Based on the data we have, measured and modeled flux agree closely when the model coefficients  $a$ ,  $b$ ,  $c$ ,  $d$  and  $e$  are calculated individually for each year.

The highest parameter weight has friction velocity  $u^*$ , the lowest - relative humidity  $rRH$ . In most cases relative humidity and air pressure have a converse effect on methane emission (parameter value  $< 1.00$ ).

During the error assessment of 9 models for the years of 2009 – 2017 (Figure 10) reasonably good agreement between measured and modeled values was found for the year 2014 ( $rad=33\%$ ). The models M-2009 (the best fit for 2009 year data) and M-2010 are also characterized by low values of  $rad$  (29% and 19% respectively), but a probable reason for this is small amount of data for these years (lack of data for June and July). It seems quite reasonable that the model parameters for the year 2014 (M-2014) could give a good fit for the rest years. The model M-2014 was applied to test our hypothesis; relative average deviations of the fit residuals were

Table 3: Individual methane flux model coefficients for 2009-2017 (M-2009 - M-2017).

Year	Model	a (intercept)	b ( $u^*$ )	c ( $T_{s7}$ )	d (rRH)	e ( $P_a$ )
2009	M-2009	0.010	2.99	1.38	1.00	0.82
2010	M-2010	0.012	2.14	1.24	1.36	0.91
2011	M-2011	0.005	4.21	4.04	2.95	0.94
2012	M-2012	0.009	3.08	2.06	2.10	1.08
2013	M-2013	0.017	7.14	2.49	0.66	1.07
2014	M-2014	0.019	2.50	3.11	0.46	0.87
2015	M-2015	0.004	2.37	2.26	2.60	1.04
2016	M-2016	0.016	1.61	0.62	0.37	0.83
2017	M-2017	0.013	3.13	2.65	0.66	0.83

estimated for the M-2014 and for each yearly model individually (Table 4).

This hypothesis was rejected because of relative average deviations calculated for the M-2014 fit residuals for other years data are apparently higher than those of individually fitted models. This has led us to conclude to use different coefficients for each year, because this way the models are more precise, when they are fitted individually.

Nevertheless, *rad* values for yearly models fitted individually are relatively high (61-76% for 2015-2017), which may suggest that our FCH<sub>4</sub> model is not universal. It is presumably caused by different data quality and availability from year to year producing errors, which is quite hard to take into account and mitigate them (e.g. for the 2009, 2010, 2013, 2016 years). Despite this, we assume constructed FCH<sub>4</sub> model as a general one and appropriate for further analysis based on a set of variables with the highest parameter weights. The main reason to assume the FCH<sub>4</sub> model reliable for the general assessment of CH<sub>4</sub> flux dynamics is relatively close agreement between measured and modeled monthly average CH<sub>4</sub> fluxes (confidence interval  $1\sigma$ ). Most of monthly averages are within the confident intervals (Figure 11), even for the years characterized with low variance (June 2014; July 2010, 2015, 2016; August 2009, 2010, 2014). However, there are two exceptions: for July 2009 and August 2013, where over- and underestimations were caused by the lack of data (Figure 9). This months should be not taken into account.

Table 4: Relative average deviation of the fit residuals for individual models and for the model M-2014.

Year	Individual model	M-2014
2009	29%	33%
2010	19%	22%
2011	51%	56%
2012	47%	52%
2013	59%	63%
2014	33%	33%
2015	61%	64%
2016	76%	86%
2017	63%	65%

According to our FCH<sub>4</sub> model the highest June fluxes are modeled for the years of 2010 (19.5  $mg/m^2 d$ ) and 2012 (18.2  $mg/m^2 d$ ), but there is no measured data to prove it. The remaining years had rather similar emission during June estimated as 9 – 14  $mg/m^2 d$ . In general June was characterized by the lowest emission in comparison with July and August for each year.

During July methane emission shows generally an increase. The highest July flux was observed for 2012 (measured 27  $mg/m^2 d$ ; modeled 24.5  $mg/m^2 d$ ); 2010, 2011 and 2013 had also relatively high methane flux. The years of 2014 and 2015 were characterized by the lowest emission during July (Figure 11).

Our FCH<sub>4</sub> model demonstrates poor agreement for August fluxes, they are noticeably underestimated for 2011, 2012 and 2013. Nevertheless, these years also demonstrate the highest average August emission (measured 27 – 30  $mg/m^2 d$ ; modeled 21 – 25  $mg/m^2 d$ ).

There is still a gap for June 2009, July and August 2013 (partly) and August 2016, due to lack of methane and meteorological measurements (Figure 9).

Table 5: Cumulative CH<sub>4</sub> flux for whole summer season for the years of 2009-2017.

Year	2009	2010	2011	2012	2013	2014	2015	2016	2017
Cumulative CH <sub>4</sub> flux, $g/m^2$	1.29	1.92	1.61	2.07	1.65	1.36	1.30	0.92	1.28

Cumulative CH<sub>4</sub> fluxes were calculated for each summer season. The highest flux values are obtained for 2010 and 2012 years (1.92 and 2.07 g/m<sup>2</sup> for the whole summer season, respectively). The lowest values obtained for the years of 2009 and 2016 are not reliable due to lack of measured data.

There is no indication that CH<sub>4</sub> emission exhibits increase during last 9 years in this region. According the graph (Figure 8) cumulative summer CH<sub>4</sub> fluxes for the years 2010-2013 is relatively higher than those for 2014-2017. It appears that CH<sub>4</sub> flux time series gap-filled with the model developed in the current study does not demonstrate any emission increase. On the other hand, monthly averages CH<sub>4</sub> fluxes demonstrate no clear evidence of emission fall. Considering this, it is plausible that there is no solid indication that methane emission continuously increases or decreases during the period 2009-2017. The seasonal CH<sub>4</sub> emission rate alters from year to year and shows inter-annual fluctuations.

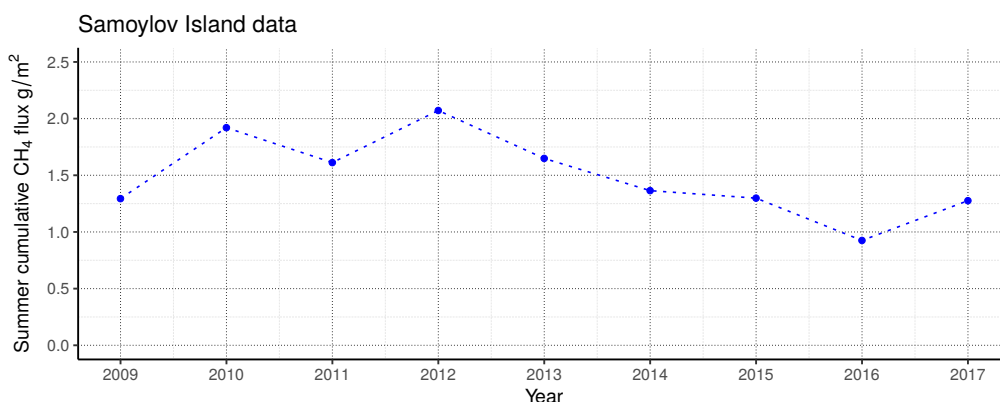


Figure 8: Cumulative CH<sub>4</sub> flux for whole summer season for the years of 2009-2017.

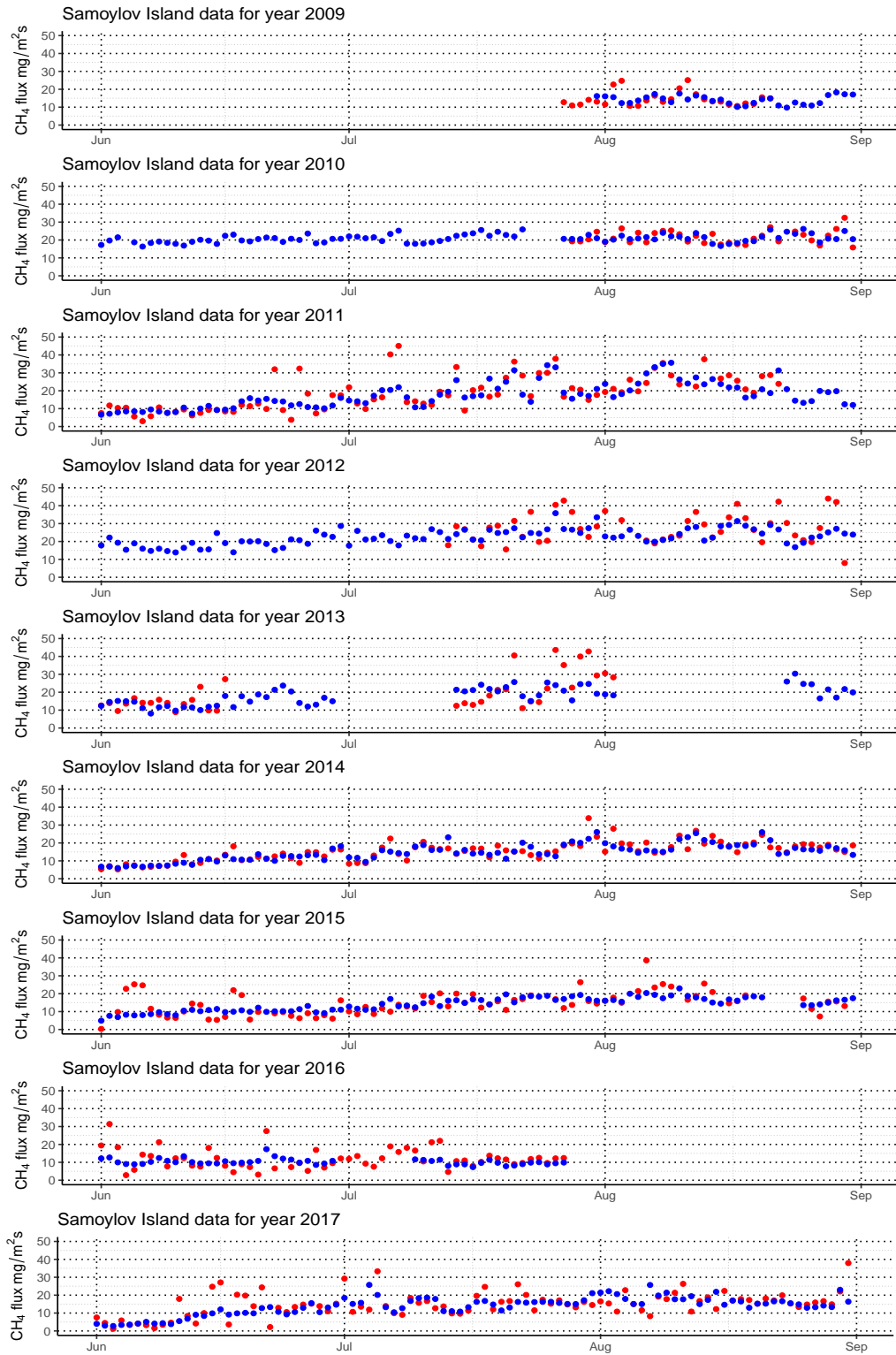


Figure 9: Gap-filling: integrated methane fluxes over the summer months 2009-2017 (red dots are the measured flux, blue dots are the modeled flux).

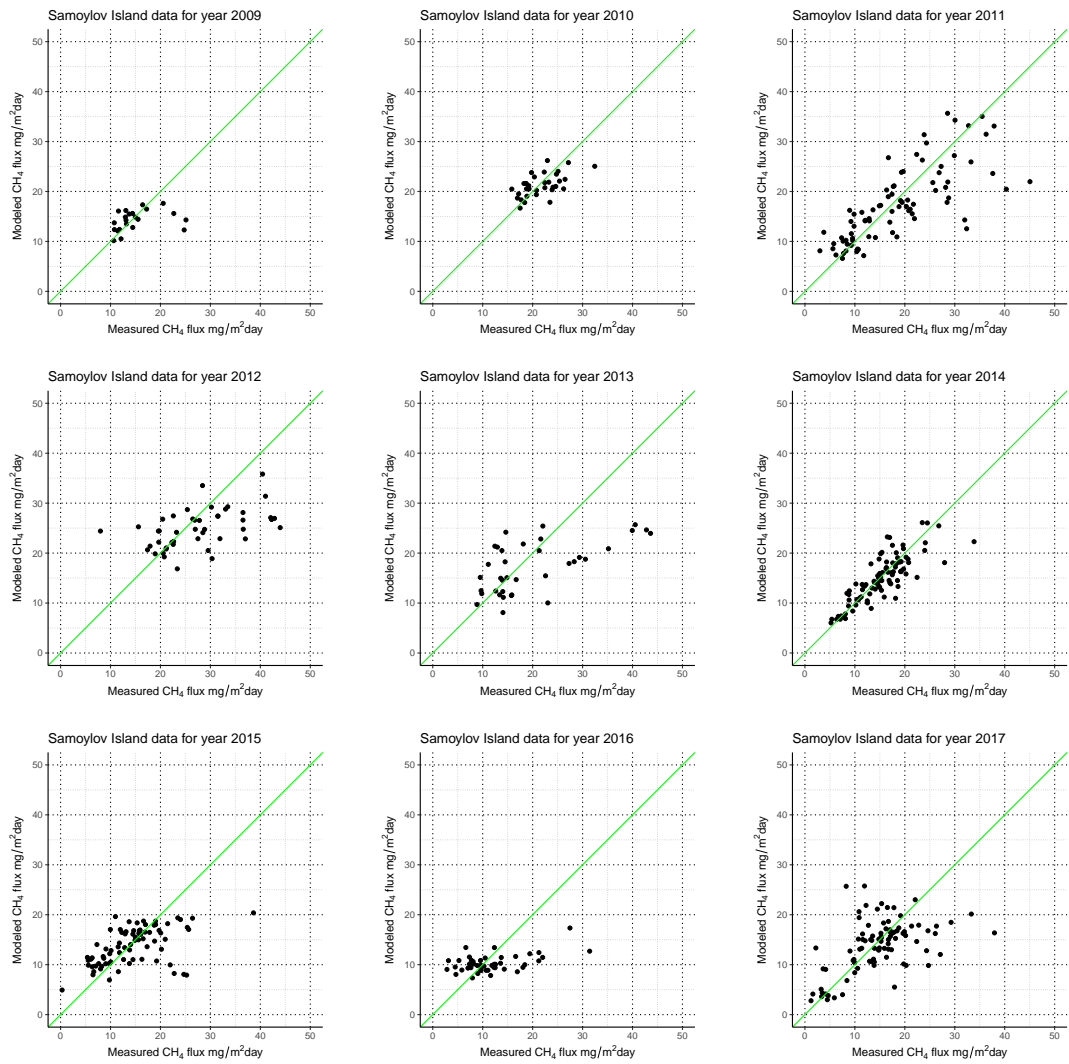


Figure 10: FCH<sub>4</sub> model assessment: agreement between measured and modeled fluxes.

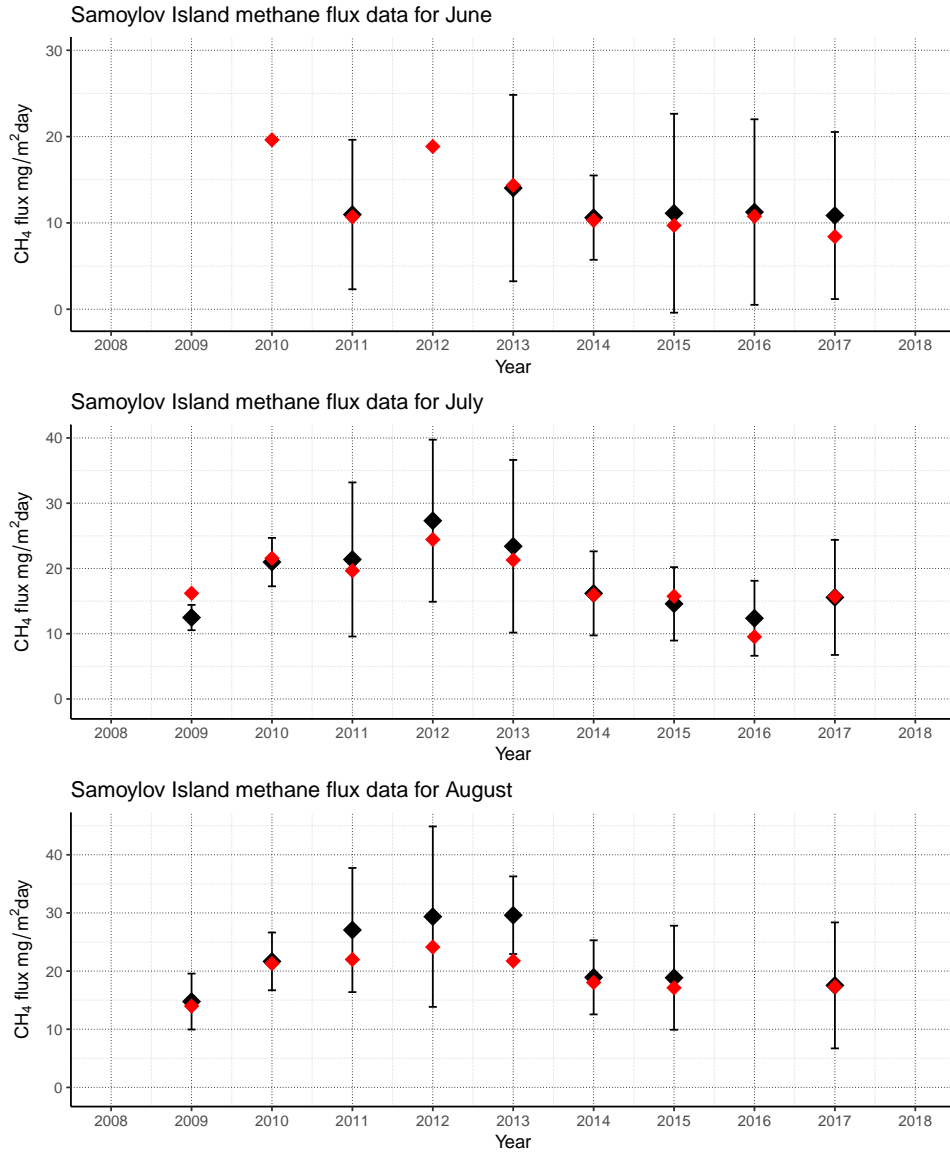


Figure 11: Integrated monthly average methane fluxes for the period of 2009-2017 (measured CH<sub>4</sub> fluxes (with a confidence interval of 1 $\sigma$ , statistically calculated) are coloured with black; modeled fluxes are coloured with red.

## 4 Discussion

This study is dedicated to inter-annual methane flux dynamics in polygonal tundra landscape, Siberian Arctic. The investigation period covers nine years with a focus on summer months. The period includes a variety of environmental conditions, which sometimes led to equipment failures, which in turn produced gaps in measured time series. These gaps in time series of different environmental parameters occur during random time periods from year to year, making the inter-annual analysis quite complicated. The most challenging problem is to unify a flux model so it would fit in general for all years. During this work we have not find any reliable way to do it and have used different coefficient sets for the  $F_{CH_4}$  models for each year. The discrepancies in the results of inter-annual analysis led us to conclude we have not taken into account some significant parameters (e.g. water table position, active layer thickness, organic acid concentration, etc.), due to lack of measured parameters in the database we used.

A number of previous studies reported the same approach to model the methane flux. A  $CH_4$  flux model proposed by Friberg et al. (2000) includes soil temperature, water table position and active layer thickness (for high-arctic fen area, Greenland). Wille et al. (2008) have reported flux model following the above-mentioned approach, but they deliberately excluded water table position and soil thaw depth, due to absence of correlation between  $CH_4$  fluxes and these parameters. Sachs et al. (2008) also found no correlation for water table position and soil thaw depth as Wille et al. (2008), and improved their model with air pressure (both studies reported data from Samoylov Island, Lena River Delta). One of the most interesting studies was reported by Christensen et al. (2003) at sites in Greenland, Iceland, Scandinavia and Siberia, where soil temperature and microbial substrate availability (organic acid concentration in peat water) combined explained almost 100% of the variations in mean annual methane emission. Though, this study relies on automatic chamber measurements and some researchers assume, that close coupling of  $CH_4$  fluxes and atmospheric parameters make enclosure-based method's reliability questionable.

During this work four environmental variables were identified as a  $CH_4$  drivers, which are friction velocity, soil temperature, air pressure and relative humidity.

Friction velocity, or near-surface atmospheric turbulence, closely correlates with



horizontal wind speed and was identified as being the most significant  $\text{CH}_4$  emission driver in polygonal tundra landscape. Increase of atmospheric turbulence could lead to aeration and short-time flushing of the  $\text{CH}_4$  stored in low moss-canopy layer during the windless period (Sachs et al., 2008). Close relationship between methane emission and near-surface atmospheric turbulence is also appears to be due to high surface coverage of water bodies in the study site. It is widely accepted, that the turbulent and diffusive water-atmosphere transport is controlled by the wind speed. There are three main pathway of methane from the water-logged areas and water bodies (Figure 1), and one of them is bubble ebullition. Recent studies reported field observations of  $\text{CH}_4$  ebullition and considered water bodies to be significant contributor to the ecosystem methane release (Walter et al., 2006). Bubble ebullition occurs in water bodies, such as lakes, and inundated soils (e.g. wet polygon centers) and is influenced not only by atmospheric turbulence, but also by air pressure. We find this dependence during the present modeling, it also confirms the modeling results by Sachs et al. (2008). They reported, that ebullition is a result of decreasing atmospheric pressure which boosts a release of free-phase gas. The  $\text{CH}_4$  emission peaks are well-correlated with decreases of air pressure and high values of friction velocity.

The next environmental parameter we have included to the  $\text{FCH}_4$  model is relative humidity, which is closely coupled with precipitation. This parameter influences the soil moisture and methanogenesis. With an increase of soil moisture the methane oxidation rate decreases, hence  $\text{CH}_4$  emission becomes higher (Semenov et al., 2009). The relationship of  $\text{CH}_4$  emission and soil temperature based on a fundamental dependence of temperature and soil microbiological activity. Almost all studies modeled  $\text{CH}_4$  flux include soil temperature in a model equation (Mastepanov et al., 2013; Wille et al., 2008; Sachs et al., 2008; Christensen et al., 2003; Friborg et al., 2000). However, this parameter is a bit questionable to include as a driver for early-summer emission, when soil is frozen, but measured  $\text{CH}_4$  fluxes are high. This discrepancy was mentioned in works by Sachs et al. (2008) and Mastepanov et al. (2013), who explained the June emission as a consequence of snow melting, which makes methane, previously trapped in lakes and ponds ice and snow coverage, be released. There is a clear indication that the main role in the process of  $\text{CH}_4$  release plays air temperature instead of soil temperature.

Despite of absence of detected direct correlation between methane fluxes and air temperature in our analysis using stepwise regression procedure, there are years with relatively low air temperature (2014-2017, Figure 6) which correspondingly have low CH<sub>4</sub> fluxes (Figure 8). It is feasible to link the air temperature and the soil temperature, which is well-correlated with the CH<sub>4</sub> flux. On a long-term scale these parameters must be connected, though their short-term variations are not linked directly. It appears that air temperature has indirect effect on CH<sub>4</sub> emission clearly seen in whole summer averages.

It should be noted that there are two processes, which are not necessary coupled: methane production and methane emission (actual gas release to the atmosphere). While methane production closely depends on soil temperature, methane release triggered by meteorological conditions. This decoupling occurs on short time scales. Methane produced by soil microorganisms can be stored in soil and sediments during calm periods and then emitted to the atmosphere when the near-surface turbulence increases.

With a growing concern to climate change Arctic regions became a focus of attention of scientists from all over the world. There is large number of studies dedicated to greenhouse gas emission from high arctic latitudes. The continued air temperature rise is expected to lead to deepening of active layer, hence it makes previously frozen organic matter available for methanogenic bacteria.

In our study we have not detected any increase of CH<sub>4</sub> emission rate over the last nine years. The changes of cumulative flux value are mostly annual fluctuations and do not show a long-term trend. Using our FCH<sub>4</sub> model we can not estimate or predict methane emission for the future years. Based on long-term methane flux and meteorological observations forecast model could be created to predict the future emission, but such simulations could be quite complicated due to many ways to introduce errors in assessment of non-linear dependent process. Moreover, each particular model may work only for exact place and time, otherwise the model could be not accurate enough for precise analysis.

## 5 Conclusions

The most correlated drivers of methane emission were identified as friction velocity, soil temperature, air pressure and relative humidity (in the descending order of model parametric weight).

Cumulative CH<sub>4</sub> fluxes were found to be from 1.28 g/m<sup>2</sup> (2017) to 2.07 g/m<sup>2</sup> (2012); the period of 2010 – 2013 was characterized by relatively high emission in comparison with the following period of 2014 – 2017. Monthly averages of June fluxes showed the lowest rates for whole investigation period, whereas July fluxes demonstrated to be relatively high ones.

Nevertheless, no clear indication of upward or downward trend in methane emission time series was found for the investigation period 2009 – 2017. It seems that CH<sub>4</sub> emission demonstrates annual fluctuation influenced by a variety of environmental parameters; the coefficient set which is the most favorable for each year model as most influential alters from year to year.

The results of this study led us to conclude that methane flux model for Samoylov Island has to include not only meteorological parameters (which control the emission process), but also parameters which control CH<sub>4</sub> production (physical and chemical/biochemical parameters of soil). We proved during our analysis that a model based mostly on meteorological parameters is not precise enough.

However FCH<sub>4</sub> model has a practical significance, it is possible to use the model as a tool for the methane flux data conditioning (rough gap-filling) for the future measurements. It has much more stability than any generic interpolation techniques, especially due to the fact that methane measurements in the database we used contain large amount of noise and boundary points should not be used as an interpolation base.

## 6 Acknowledgement

I would first like to thank Dr. Lars Kutzbach, Professor for soils in the climate system, Hamburg University. I wish to express my sincere thanks for valuable guidance and encouragement extended to me and providing me with all the necessary materials and data for the research.

A very special gratitude goes out to Prof. Dr. Eva-Maria Pfeiffer, Tim Eckhardt and the KoPf – Kohlenstoff im Permafrost Project for helping and providing the funding for the study semester in Hamburg University, where this work was started. I am also grateful to Spyridon Karamichail and David Holl, students of Hamburg University and members of working group of Prof. Dr. Lars Kutzbach. I am extremely thankful and indebted to them for sharing expertise in data processing and programming, and helping to me with all the tasks I had.

I take this opportunity to express my gratitude to Philipp Oleynik, Researcher at Faculty of Science and Engineering, University of Turku, Finland, for supporting me for everything, and especially for consulting me about complicated mathematical and programming stuff. I can not thank him enough for encouraging me throughout this experience.

I would also like to acknowledge my scientific consultant Dr. Svetlana Evgrafova. I am gratefully indebted to her for very valuable comments on this work.

And finally, last but by no means least, also I would like to express my special appreciation and thanks to my scientific supervisor Dr. Irina Fedorova.

## Bibliography

- Are, F. and Reimnitz, E. (2000). An overview of The Lena River Delta setting: Geology, tectonics, geomorphology, and hydrology. 16:1083–1093.
- Arora, V. K., Berntsen, T., Biastoch, A., Bousquet, P., Bruhwiler, L., Bush, E., Chan, E., Christensen, T. R., Dlugokencky, E., Fisher, R. E., France, J., Gauss, M., Höglund-Isaksson, L., Houweling, S., Huissteden, K., Janssens-Maenhout, G., Karion, A., Kiselev, A., Koven, C. D., Kretschmer, K., Kupiainen, K., Kupperberg, J. M., Laurila, T., Li, G., Lowry, D., Melton, J., Miller, J., Nisbet, E. G., Olivé, D. J., Panieri, G., Parmentier, F.-J. W., Plummer, D. A., Rao, S., Sachs, T., Shepherd, M., Silyakova, A., Søvde, O. A., Sweeney, C., Taylor, C., Thomson, A., White, J. W., Worthy, D., and Zhang, W. (2015). *AMAP Assessment 2015: Methane as an Arctic Climate Forcer*. AMAP Assessment Report. Arctic Monitoring and Assessment Programme (AMAP), Oslo, Norway.
- Aubinet, M., Vesala, T., Papale, D., Aubinet, M., Vesala, T., and Papale, D. (2013). *Eddy Covariance. A Practical Guide to Measurement and Data Analysis*. Springer Atmospheric Sciences.
- Boike, J., Kattenstroth, B., Abramova, K., Bornemann, N., Chetverova, A., Fedorova, I., Fröb, K., Grigoriev, M., Grüber, M., Kutzbach, L., Langer, M., Minke, M., Muster, S., Piel, K., Pfeiffer, E.-M., Stoof, G., Westermann, S., Wischniewski, K., Wille, C., and Hubberten, H.-W. (2013). Baseline characteristics of climate, permafrost and land cover from a new permafrost observatory in The Lena River Delta, Siberia (1998 – 2011). *Biogeosciences*, 10(3):2105–2128.
- Boike, J., Wille, C., and Abnizova, A. (2008). Climatology and summer energy and water balance of polygonal tundra in The Lena River Delta, Siberia. *Journal of Geophysical Research: Biogeosciences*, 113(G3):n/a–n/a. G03025.
- Bousquet, P., Ringeval, B., Pison, I., Dlugokencky, E. J., Brunke, E.-G., Carouge, C., Chevallier, F., Fortems-Cheiney, A., Frankenberg, C., Hauglustaine, D. A., Krummel, P. B., Langenfelds, R. L., Ramonet, M., Schmidt, M., Steele, L. P., Szopa, S., Yver, C., Viovy, N., and Ciais, P. (2012). Source attribution of

- the changes in atmospheric methane for 2006-2008. *Atmospheric Chemistry and Physics*, 12(19):9381–9382.
- Burba, G. (2013). *Eddy Covariance Method for Scientific, Industrial, Agricultural and Regulatory Applications: A Field Book on Measuring Ecosystem Gas Exchange and Areal Emission Rates*. LI-COR Biosciences.
- Chesworth, W. (2008). *Encyclopedia of Soil Science*. Springer Netherlands.
- Christensen, T. R., Ekberg, A., Ström, L., Mastepanov, M., Panikov, N., Öquist, M., Svensson, B. H., Nykänen, H., Martikainen, P. J., and Oskarsson, H. (2003). Factors controlling large scale variations in methane emissions from wetlands. *Geophysical Research Letters*, 30(7):n/a–n/a. 1414.
- Christensen, T. R., Prentice, I. C., Kaplan, J., Haxeltine, A., and Sitch, S. (1996). Methane flux from northern wetlands and tundra. *Tellus B*, 48(5):652–661.
- Demyanov, V. V. and Saveleva, E. A. (2000). *Geostatistika: teoriya i praktika*. Nauka.
- Denman, K., Brasseur, G., Chidthaisong, A., Ciais, P., Cox, P., Dickinson, R., Hauglustaine, D., Heinze, C., Holland, E., Jacob, D., Lohmann, U., Ramachandran, S., da Silva Dias, P., Wofsy, S., and Zhang, X. (2007). Couplings between changes in the climate system and biogeochemistry. In *Climate Change 2007: The Physical Science Basis. Contribution of Working Group I to the Fourth Assessment Report of the Intergovernmental Panel on Climate Change*. Cambridge University Press, IPCC.
- Foken, T. and Wichura, B. (1996). Tools for quality assessment of surface-based flux measurements. 78:83–105.
- Franz, D., Koebisch, F., Larmanou, E., Augustin, J., and Sachs, T. (2016). High net CO<sub>2</sub> and CH<sub>4</sub> release at a eutrophic shallow lake on a formerly drained fen. *Biogeosciences*, 13(10):3051–3070.
- French, H. (1996). *The Periglacial Environment*. Pearson Education.

- Friberg, T., Christensen, T. R., Hansen, B., Nordström, C., and Sögaard, H. (2000). Trace gas exchange in a high-arctic valley 2. Landscape CH<sub>4</sub> fluxes measured and modeled using eddy correlation data. *Global Biogeochemical Cycles*, 14(3):715–723.
- Frolking, S., Roulet, N., and Lawrence, D. (2013). *Issues Related to Incorporating Northern Peatlands into Global Climate Models*, pages 19–35. American Geophysical Union.
- Hubberten, H.-W., Wagner, D., Pfeiffer, E. M., Boike, J., and Gukov, A. Y. (2006). The Russian-German Research Station Samoylov, Lena Delta - a key site for polar research in the Siberian Arctic. *Polarforschung*, 73(2/3):111–116.
- Hugelius, G., Strauss, J., Zubrzycki, S., Harden, J. W., Schuur, E. A. G., Ping, C.-L., Schirmer, L., Grosse, G., Michaelson, G. J., Koven, C. D., O'Donnell, J. A., Elberling, B., Mishra, U., Camill, P., Yu, Z., Palmtag, J., and Kuhry, P. (2014). Estimated stocks of circumpolar permafrost carbon with quantified uncertainty ranges and identified data gaps. *Biogeosciences*, 11(23):6573–6593.
- Jahn, M., Sachs, T., Mansfeldt, T., and Overesch, M. (2010). Global climate change and its impacts on the terrestrial arctic carbon cycle with special regards to ecosystem components and the greenhouse-gas balance. *Journal of Plant Nutrition and Soil Science*, 173(5):627–643.
- Kutzbach, L. (2006). The exchange of energy, water and carbon dioxide between wet arctic tundra and the atmosphere at The Lena River Delta, Northern Siberia.
- Kutzbach, L., Wagner, D., and Pfeiffer, E. (2003). Effect of microrelief and vegetation on methane emission from wet polygonal tundra, Lena Delta, Northern Siberia. *Biogeochemistry*, pages 341–362.
- Mastepanov, M., Sigsgaard, C., Tagesson, T., Ström, L., Tamstorf, M. P., Lund, M., and Christensen, T. R. (2013). Revisiting factors controlling methane emissions from high-arctic tundra. *Biogeosciences*, 10(7):5139–5158.
- Mauder, M. and Foken, T. (2015). Documentation and instruction manual of the eddy-covariance software package tk3. 62:62.

- Prather, M., D. Holmes, C., and Hsu, J. (2012). Reactive greenhouse gas scenarios: Systematic exploration of uncertainties and the role of atmospheric chemistry. 39:9803–.
- Prather, M., Ehhalt, D., Dentener, F., Derwent, R., and Grubler, A. (2001). Atmospheric chemistry and greenhouse gases. In *Climate Change 2001: The Scientific Basis, Third Assessment Report*. Working Group I of the Intergovernmental Panel on Climate Change, IPCC.
- R Core Team (2013). *R: A Language and Environment for Statistical Computing*. R Foundation for Statistical Computing, Vienna, Austria.
- Sachs, T., Giebels, M., Wille, C., Kutzbach, L., and Boike, J. (2008b). Methane emission from Siberian wet polygonal tundra on multiple spatial scales: Vertical flux measurements by closed chambers and eddy covariance, Samoylov Island, Lena River Delta.
- Sachs, T., Wille, C., Boike, J., and Kutzbach, L. (2008). Environmental controls on ecosystem-scale CH<sub>4</sub> emission from polygonal tundra in The Lena River Delta, Siberia. *Journal of Geophysical Research: Biogeosciences*, 113(G3):n/a–n/a. G00A03.
- Semenov, M. V., Zadorozhniy, A. N., Khodzhaeva, A., and Semenov, V. M. (2009). Production, consumption, and emission of greenhouse gases in the soil. *Agrokhimia*, 2010:75–92.
- Soil Survey Staff (1998). *Keys to Soil Taxonomy*. United States Department of Agriculture, Natural Resources Conservation Service.
- Solomon, S. (2007). *Climate change 2007-the physical science basis: Working group I contribution to the fourth assessment report of the IPCC*, volume 4. Cambridge University Press.
- Walter, B. P., Heimann, M., and Matthews, E. (2001). Modeling modern methane emissions from natural wetlands: 1. Model description and results. *Journal of Geophysical Research: Atmospheres*, 106(D24):34189–34206.



- Walter, K., Zimov, S., Chanton, J., Verbyla, D., and Chapin III, F. S. (2006). Methane bubbling from Siberian thaw lakes as a positive feedback to climate warming. *Nature*, 443:71–5.
- Webb, E. K., Pearman, G. I., and Leuning, R. (1980). Correction of flux measurements for density effects due to heat and water vapour transfer. *Quarterly Journal of the Royal Meteorological Society*, 106(447):85–100.
- Whalen, S. (2005). Biogeochemistry of methane exchange between natural wetlands and the atmosphere. 22.
- Whiting, G. J. and Chanton, J. P. (2001). Greenhouse carbon balance of wetlands: methane emission versus carbon sequestration. *Tellus B*, 53(5):521–528.
- Wilczak, J., Oncley, S., and Stage, S. (2001). Sonic anemometer tilt correction algorithms. *Boundary-Layer Meteorology*, 99:127–150.
- Wille, C., Kutzbach, L., Sachs, T., Wagner, D., and Pfeiffer, E.-M. (2008). Methane emission from Siberian arctic polygonal tundra: eddy covariance measurements and modeling. *Global Change Biology*, 14(6):1395–1408.
- Zhang, T., Barry, R., Knowles, K., A. Heginbottom, J., and Brown, J. (2008). Statistics and characteristics of permafrost and ground-ice distribution in the Northern Hemisphere. 31:47–68.
- Zhang, Y., Sachs, T., Li, C., and Boike, J. (2012). Upscaling methane fluxes from closed chambers to eddy covariance based on a permafrost biogeochemistry integrated model. 18.
- Zhuang, Q., Melillo, J. M., Kicklighter, D. W., Prinn, R. G., McGuire, A. D., Steudler, P. A., Felzer, B. S., and Hu, S. (2004). Methane fluxes between terrestrial ecosystems and the atmosphere at northern high latitudes during the past century: A retrospective analysis with a process-based biogeochemistry model. *Global Biogeochemical Cycles*, 18(3):n/a–n/a. GB3010.
- Zona, D., Gioli, B., Commane, R., Lindaas, J., Wofsy, S. C., Miller, C. E., Dinardo, S. J., Dengel, S., Sweeney, C., Karion, A., Chang, R. Y.-W., Henderson, J. M.,

Murphy, P. C., Goodrich, J. P., Moreaux, V., Liljedahl, A., Watts, J. D., Kimball, J. S., Lipson, D. A., and Oechel, W. C. (2016). Cold season emissions dominate the arctic tundra methane budget. *Proceedings of the National Academy of Sciences*, 113(1):40–45.